

<https://doi.org/10.1038/s43247-024-01260-7>

# Identification of reliable locations for wind power generation through a global analysis of wind droughts

Check for updates

Enrico G. A. Antonini <sup>1,2,3</sup> ✉, Edgar Virgüez <sup>1</sup>, Sara Ashfaq <sup>1,4</sup>, Lei Duan <sup>1,5</sup>, Tyler H. Ruggles <sup>1</sup> & Ken Caldeira <sup>1,6</sup>

Wind droughts, or prolonged periods of low wind speeds, pose challenges for electricity systems largely reliant on wind generation. Using weather reanalysis data, we analyzed the global distribution of and trends in wind droughts using an energy deficit metric that integrates the depth and duration of wind droughts. We identified regions with high power densities, low seasonal variability, and limited weather fluctuations that favor wind power generation, such as the American Midwest, Australia, the Sahara, Argentina, Central Asia, and Southern Africa. Northwestern Europe has high power densities but experiences more frequent and prolonged wind droughts due to higher weather variability. We found little evidence for strong trends in wind droughts over recent decades in most places. Rather, the most severe wind droughts in many places occurred before wind power substantially penetrated power systems, which suggests that historical weather data can be useful in designing reliable wind-reliant electricity systems.

Wind power is one of the critical low-carbon energy sources that is expected to play a substantial role in decarbonizing electricity generation. In 2021, about 6.5% of the world's electricity was generated from wind<sup>1</sup>; however, under some energy transition scenarios<sup>2</sup>, onshore and offshore wind will provide more than one-third of global electricity needs by 2050. In 2021, multiple countries had a substantial share of electricity generated from wind, much greater than the world's average, including Denmark (48%), Uruguay (32%), Ireland (31%), Lithuania (28%), Portugal (27%), Spain (23%), United Kingdom (21%), and Germany (20%). Before 2000, no country had a share greater than 10%; until 2007, only Denmark had a share greater than 10%<sup>3</sup>.

As we transition to larger penetrations of this highly variable renewable energy source into our power systems, prolonged periods of low wind speeds, herein referred to as “wind droughts”, can have severe consequences for electricity systems that largely rely on wind. For example, Northwestern Europe experienced a long period of low wind speeds through the summer and early autumn of 2021<sup>4,5</sup>. This wind drought further strained the European electricity system, which was already affected by depleted natural gas reserves and increased natural gas prices. In 2015, the Western and Southern United States experienced the lowest recorded windiness period in terms of geographic extent and longevity since 1979 (the beginning of widespread satellite measurements)<sup>6,7</sup>. This event severely impacted wind power

generation in the Western United States, where at the time wind power generated ~6% of electricity in the Western Interconnection<sup>8</sup>. In 2020, wind power in India, with about a 4% share in the electricity mix, generated much lower electricity than expected during the peak summer monsoon (about 24% lower energy generation compared to 2019)<sup>9</sup>. These events show how the increasing use of this intermittent source can exacerbate the exposure of national power systems to meteorological variability, potentially requiring emergency intervention by the system operators.

It is important in energy system planning to understand the severity and distribution of wind droughts and their trends in historical records. The characterization of wind variability and droughts is commonly conducted with intensity–duration–frequency analyses to quantify the occurrence of continuous periods of wind speeds lower than a given threshold<sup>10,11</sup>. For example, durations ranging from 1 h to 20 days are typically considered, showing that sustained 10- to 20-day periods of low levels of wind generation could have return periods of around 10 years. Such analyses, however, do not capture the combined effect of consecutive wind droughts that are interrupted only by a few hours of normal wind generation. These combined scarcity periods can be highlighted only by integrating the energy deficit over a much longer period than the one associated with a single wind drought. For example, Ruhnan and Qvist<sup>12</sup> analyzed storage requirements as

<sup>1</sup>Department of Global Ecology, Carnegie Institution for Science, Stanford, CA, USA. <sup>2</sup>CMCC Foundation - Euro-Mediterranean Center on Climate Change, Lecce, Puglia, Italy. <sup>3</sup>RFF-CMCC European Institute on Economics and the Environment, Milano, Lombardia, Italy. <sup>4</sup>Electric Power Research Institute (EPRI), Palo Alto, CA, USA. <sup>5</sup>Orca Sciences LLC, Kirkland, WA, USA. <sup>6</sup>Breakthrough Energy, Kirkland, WA, USA. ✉e-mail: [enrico.antonini@cmcc.it](mailto:enrico.antonini@cmcc.it)

a proxy for the energy deficit created by multiple scarce periods of both wind and solar generation that closely follow each other. This approach has the potential to reveal combined energy deficits that span several weeks and properly inform energy system planners about the real impact of prolonged, consecutive periods of low generation from wind or other weather-dependent energy sources.

In characterizing the severity and distribution of wind droughts, it is also important to consider and quantify how much change there could be as a result of a changing climate. The effects of climate change on winds have been investigated in the past, but evidence for a significant change has not been conclusive<sup>13</sup>. Some studies suggest that by the end of the twenty-first century, energy density may increase in Northern Europe<sup>14,15</sup> and decrease in the Southeast<sup>16,17</sup>. An analysis of winds over the contiguous United States indicates a tendency toward reduced values of annual wind speeds<sup>18</sup>. These changes are consistent with a global analysis of projected future surface wind speeds that highlights a decrease across the mid-latitudes of the northern hemisphere and an increase across the tropics and subtropics of the southern hemisphere<sup>19</sup>. However, wind speeds projected with global climate models and regionally downscaled models show a high degree of sensitivity to the boundary conditions<sup>20,21</sup>, leading to substantial uncertainties of wind speed changes and limiting their usefulness for energy system planners<sup>22</sup>.

In this study, we conduct a historical analysis of the global distribution of and trends in wind droughts to investigate whether recent wind drought events should be attributed to climate variability or long-term trends. We analyze the ERA5 weather reanalysis (the fifth-generation atmospheric reanalysis of the global climate by the European Center for Medium-Range Weather Forecasts) for the period from 1979 through 2022, using an energy deficit metric that integrates the depth and duration of wind droughts over periods that may contain brief intervals with high winds. Here, we consider periods spanning a single calendar year each, where multiple events of lower than-expected wind generation can occur. By considering the wind power density time series at each grid cell of the reanalysis product, we examine the climatological mean seasonal cycle of the wind power density, which we call “seasonal variability”; departures from the climatological mean seasonal cycle of the wind power density, which we call “weather variability”; and the wind droughts (see Methods for detailed mathematical definitions). We quantify seasonal variability, weather variability, and wind droughts using an energy deficit metric that is related to the amount of storage that would be needed to overcome them. For each of these three quantities, we evaluate the aggregated impact over the considered periods, which are all one calendar year. Lastly, we analyze trends in annual mean power densities, weather variability, and wind droughts to understand potential long-term changes in wind resources. Results from the study ultimately provide a better understanding of the potential of wind power to contribute to the generation of a reliable decarbonized electricity system.

## Results

This section starts with an overview of global wind resources by showing the distribution of mean power density, seasonal variability, and weather variability around the world. Then, we quantify the distribution of these variabilities as a function of the power density. By calculating the percentile ranks of these variables for each grid cell, we show the places that are the most favorable for energy generation from wind. Lastly, we provide a historical analysis of wind droughts around the world, highlighting areas where wind droughts are more frequent and severe and where the severity of wind droughts has increased over the years.

Figure 1 shows mean wind power density (panel a), seasonal variability (panel b), and weather variability (panel c). The color scale of each map is divided according to equally spaced percentile intervals. To calculate the percentile values for each location, we sorted power density in ascending order, and the seasonal and weather variability in descending order, and then assigned each a percentile rank. A location scores a high rank if it has a high power density, a low seasonal variability or a low weather variability. The mean wind power density and mean weather variability are calculated as the average across the 44 years of data. Variabilities are plotted using the

energy deficit metric and normalized to the maximum theoretical deficit, which is one calendar year. This energy deficit metric allows us to identify regions that are characterized by low seasonal and weather variability, which in turn are more attractive for wind energy generation. In each map, the brighter the color, the better the location is for the plotted variable. To highlight regions relevant for wind energy development, only grid cells over land and coastal areas, excluding Greenland and Antarctica, are plotted (see Supplementary Fig. 1 for the division of grid cells by regions). Maps that show the distribution of each variable over the entire globe are plotted in Supplementary Fig. 2.

We find that the American Midwest, Northeastern Canada, Australia, the Sahara, Argentina, parts of Central Asia and Southern Africa, Northern Russia, and Central and Northwestern Europe have relatively high power densities, mostly in the range of 250 to 500 W m<sup>-2</sup>. Of these regions, we also find that some are characterized by high amounts of seasonal variability, such as Europe, mostly in the range of 0.15 to 0.25 (fraction of a year). Other regions, such as part of the Amazon and Eastern Russia, have low seasonal variability but relatively low power densities. Mean weather variability appears more uniform across land and coastal areas, with low variability in parts of Africa and Australia. These maps highlight the different characteristics of the wind resources present in different locations, where some have high mean power densities and low variability, but others have high mean power densities and high variability.

We show the distribution of variability as a function of the mean power density in Supplementary Fig. 3. Panels a–c, show the distribution of seasonal variability, while panels d–f show the distribution of weather variability. We separated the grid cells over land (panels a and d), over coastal areas (panels b and e), and over sea and ice sheets (panels c and f). The ice sheets include Greenland and Antarctica, which are excluded from the panels that include land areas. Most of the grid cells over land are characterized by mean power densities less than 200 W m<sup>-2</sup> and a seasonal variability with energy deficits in the range of 0.04 to 0.20 (fraction of a year), with a higher probability of being in the range of 0.08 to 0.16. Over coastal areas, mean power densities are higher and most frequent in the range of 200 to 600 W m<sup>-2</sup>, while normalized deficits associated with seasonal variability are mostly uniformly spread over the range of 0.04 to 0.20. Over sea and ice sheets, mean power densities are the highest, with most values in the range of 300 to 1500 W m<sup>-2</sup> (the windiest regions of the world are over the Indian Ocean and Antarctica). The seasonal variability over these regions is typically characterized by normalized deficits in the range of 0.04 to 0.20, with a higher probability of being in the range of 0.08 to 0.12. While the distribution of the mean power density is substantially different among land, coast, and sea, the distribution of normalized seasonal variability appears mostly in the range of 0.04 to 0.24. Weather variability is typically characterized by normalized energy deficits in the range of 0.04 to 0.16, narrower than the range of seasonal variability.

In Fig. 2, we show the minimum percentile rank across mean power density, seasonal variability, and weather variability, where low rank means less and high rank means more. In Supplementary Figs. 4–9, we show in more detail the distribution of the minimum percentile rank for each continent. This minimum percentile rank highlights regions that score a relatively high value for all three variables and can, therefore, be considered attractive for high and sustained wind energy generation. We find that the American Midwest, Northeastern Canada, Australia, the Sahara, Argentina, parts of Central Asia, and Southern Africa are the regions that have the highest minimum percentile ranks. Central and Northwestern Europe, although characterized by relatively high power densities, do not score high overall because their variability is not as low as that of the other regions previously mentioned. Regions that have a zero or close to zero value for at least one of the variables under consideration are the equatorial regions in South America, Africa, and Southeast Asia, and mountainous regions.

To show our results regarding the prevalence of wind droughts, we first plot in Fig. 3 the distribution across years of the fraction of the region affected by the most severe wind droughts. Only places on land or coastal areas with a mean power density greater than or equal to 150 W m<sup>-2</sup> are

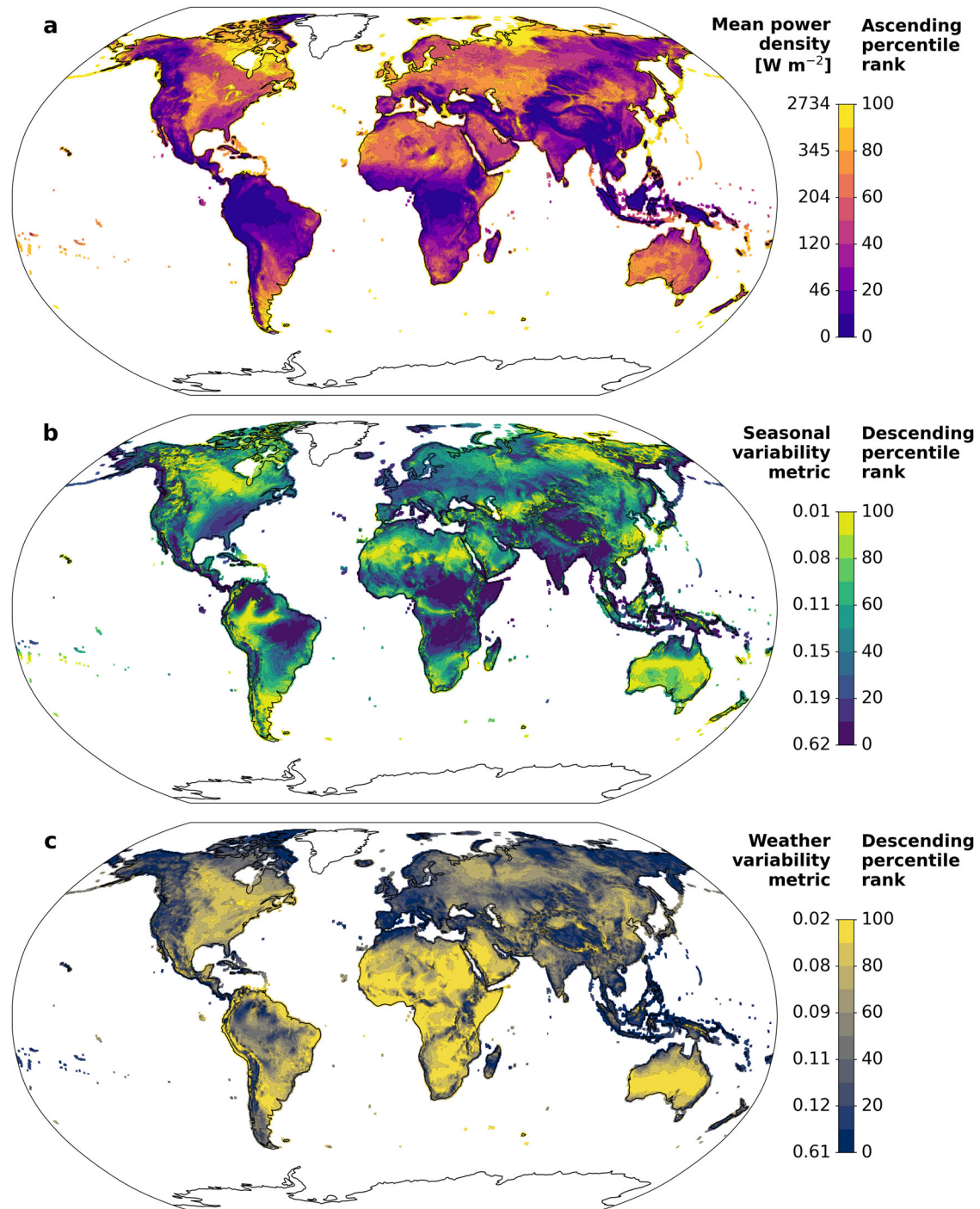


**Fig. 1 | Global distribution of power density, seasonal variability, and weather variability.** Panel a shows the mean power density, panel b the seasonal variability, and panel c the weather variability. The color scale of each map is divided according to equally spaced percentile intervals. The mean wind power density and weather variability are calculated as the average across the 44 years of data (1979–2022). Variabilities are plotted using the energy deficit metric and normalized to the

maximum theoretical deficit, which is one calendar year. Only grid cells over land and coastal areas, excluding Greenland and Antarctica, are plotted. High mean power densities, with low seasonal and weather variabilities, would tend to make a location more attractive for wind generation. Color maps in all panels are such that lighter colors indicate better quality of wind resources.

considered. Their extension accounts for ~48% of the total land and coastal areas, excluding Greenland and Antarctica. For each continent, horizontal bars show the fraction of the area in that continent that experiences the most severe wind drought in any particular year of the 44-year period under consideration. Bars in each vertical column sums to 100%. In Asia, the most severe wind droughts occurred in the late 2000s and 2010s. In North America and Oceania, the fraction of the area affected by the worst wind droughts appears to be more uniformly distributed across the years under

consideration. In South America, there is evidence of three large wind droughts in 1985, 1998, and 2016. Africa experienced most of its most severe wind droughts in the 1980s and 1990s, while its largest wind drought occurred more recently in 2010. In Europe, the most severe wind droughts occurred in the 1980s and 2010s, with the two largest events in 2009 and 2010. This figure shows that the most severe wind droughts in many places occurred well before wind power generation started to penetrate power systems.

**Fig. 2 | Areas with abundant and reliable wind power.** The map shows the minimum percentile rank across mean power density, seasonal variability, and weather variability. To indicate regions with potential for relatively strong and reliable wind generation, we give a high score if it has a high power density, a low seasonal variability, and a low weather variability, using the minimum of the percentile rankings shown in Fig. 1. Areas that this metric identifies as having good wind resources are shown in orange and red colors.

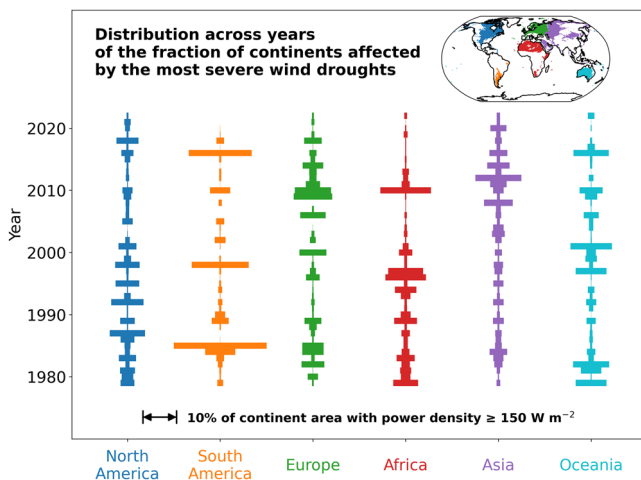
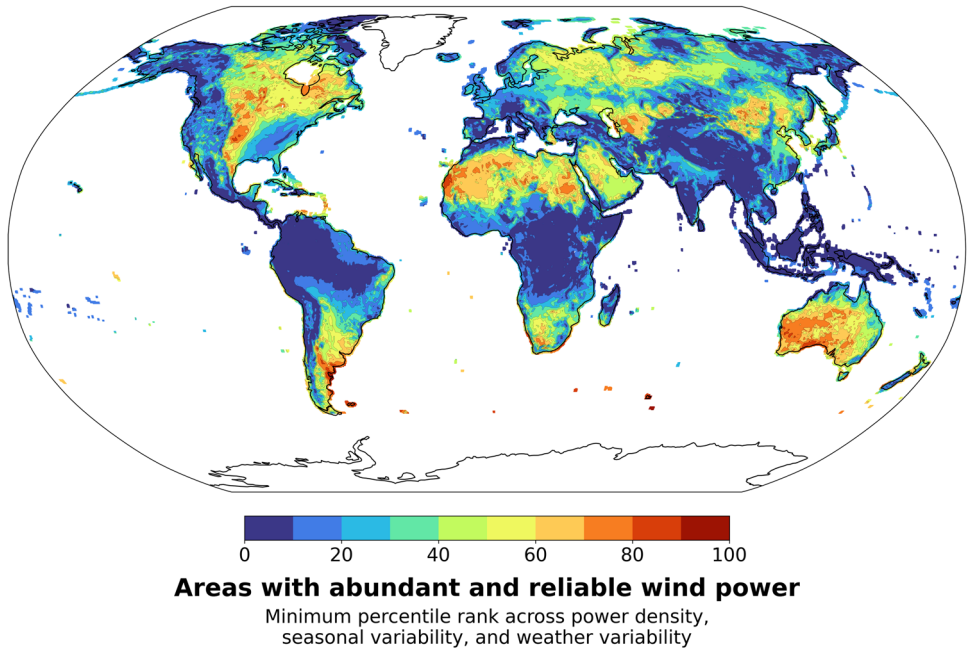


**Fig. 3 | Distribution across years of the fraction of continents affected by the most severe wind droughts.** For each continent, horizontal bars show the fraction of the area in that continent that experiences the most severe wind drought in any particular year of the 44-year period under consideration. Only places on land or coastal areas and with a mean power density greater than or equal to  $150 \text{ W m}^{-2}$  are considered. Their extension accounts for ~48% of the total land and coastal areas, excluding Greenland and Antarctica, and are illustrated in the map in the top-right corner. Bars in each vertical column sum to 100%. This figure shows that the most severe wind droughts in many places occurred before wind power generation started to penetrate power systems.

In Supplementary Fig. 10, we present more extensive results of our historical analysis of wind droughts. Panel a shows the year of the most severe wind drought, panel b shows the duration of the most severe wind drought in hours of energy deficit, and panel c shows the probability of having a year with wind droughts causing more than 400 h of deficit. Our energy deficit metric identifies in Northwestern Europe in 2010 (blue color) a wind drought deeper than the one experienced in 2021, which does not appear as one of the most severe from our analysis. In the American Midwest, extensive wind droughts occurred in the 1980s and 1990s well before wind power generation was adopted. Our energy deficit metric also captures recent wind droughts, such as the one that occurred in India in 2021 (purple color on Indian coastal areas)

or in the Western United States in 2015 (dark purple color over the coastal areas of California). The most severe wind droughts occurred over Central Asia, Northwestern Europe, the Mediterranean Sea, and Northern Canada, with lengths of a few weeks of energy deficit (2000 h are about 12 weeks). Northwestern Europe, the Mediterranean Sea, Northern Canada, and some parts of Northern Russia are among the regions with the highest probability of experiencing severe wind droughts causing more than 400 h of energy deficit (400 h are about 17 days). For example, Northwestern Europe has a probability between 60 and 80% of experiencing such an energy deficit when we consider a climatological target power generation. Regions with the lowest probability of long wind droughts include the American Midwest, the Sahara, Argentina, and Australia.

In Fig. 4, we calculate trends in power density, weather variability, and drought severity. For each grid cell, we performed a linear regression on the annual values of each variable. In this figure, we show the distribution of trends also over oceans and ice sheets to highlight potential spatial patterns. Parallel lines indicate regions where the linear regression has a  $p$ -value greater than 0.05, meaning that the trend is not statistically significant. The power density exhibits significant positive trends in some regions over the Tropics (between 0.1 and 3%), Central North America (between 0.1 and 1%), Central Africa (between 0.1 and 3%), the Amazon (between 0.3 and 3%), and the Indian Ocean (between 0.1 and 0.3%), whereas negative trends are present in Central Europe and India (between  $-0.1$  and  $-1\%$ ). Weather variability does not exhibit significant changes over the years of our analysis, except in a few small regions in North America (between  $-0.3$  and  $-1\%$ ), the Amazon (between  $-0.3$  and  $-3\%$ ), Eastern Europe (between  $-0.3$  and  $-3\%$ ), and Western Africa (between 0.3 and 3%). Changes in wind drought severity, which combine both the effect of power density and weather variability, are statistically significant and negative in some regions over the oceans in the Tropics (between  $-1$  and  $-10\%$ ), Central North America (between  $-1$  and  $-3\%$ ), the Amazon (between  $-1$  and  $-10\%$ ), and Africa (between  $-1$  and  $-10\%$ ). Increasing wind drought severity is present in India and Western Africa (between 1 and 3%). Overall, regions with statistically significant changes in wind drought severity resemble the areas with statistically significant changes in power density, suggesting its more prominent role played in contrast to changes in weather variability. Note that the percentage of land and coastal areas that have a mean wind power density greater than or equal to  $150 \text{ W m}^{-2}$  and have a statistically significant trend is 11% when considering the trend in wind power density, 4% when considering the trend in weather variability, and 7% when considering the trend in wind droughts.

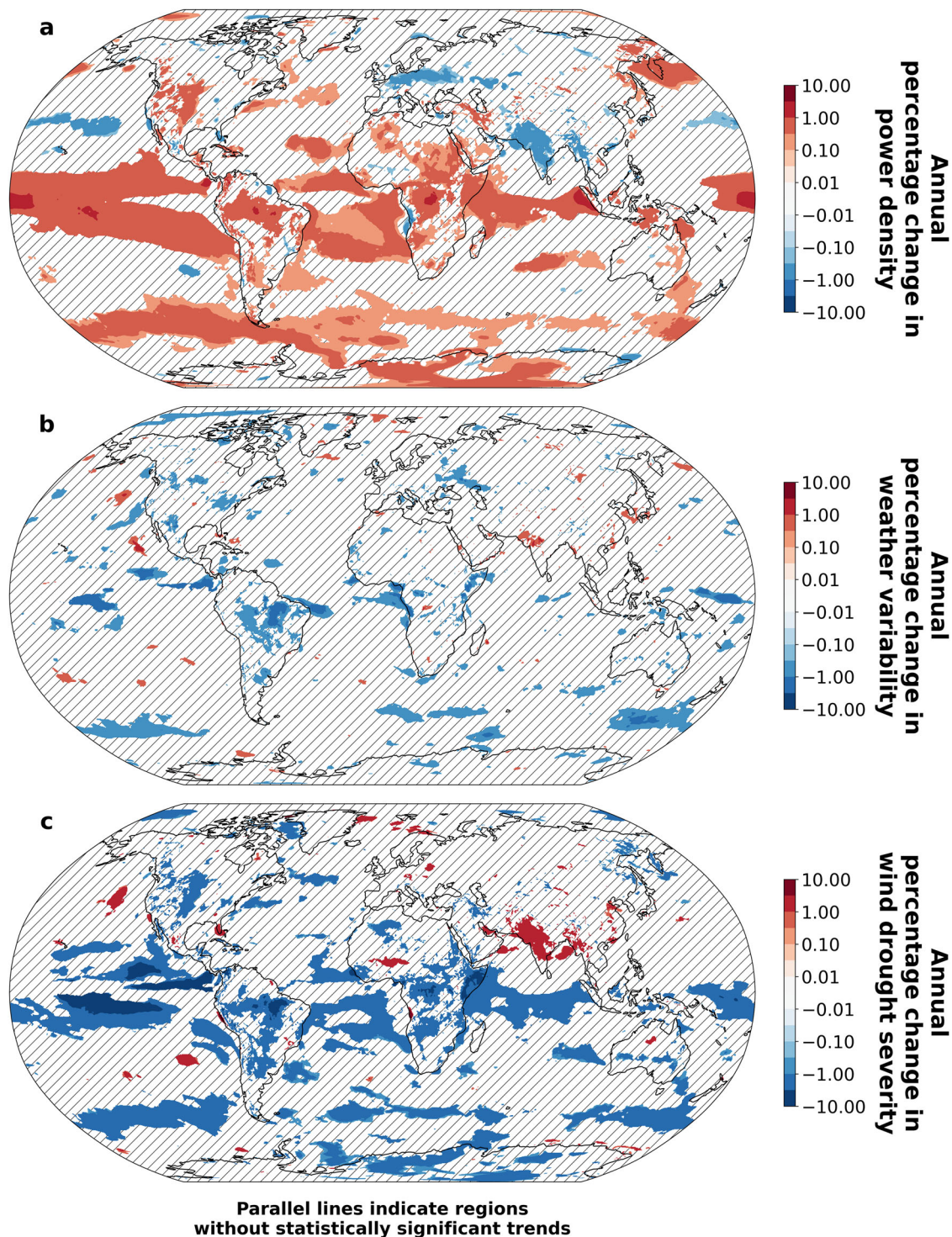


**Fig. 4 | Global trends in wind power density, weather variability, and wind drought severity.** Panel a shows trends in wind power density, panel b trends in weather variability, and panel c trends in wind drought severity. For each grid cell, we performed a linear regression on the annual values of each variable. Parallel lines on a white background indicate regions where the linear regression has a *p*-value greater than 0.05, meaning that the trend is not statistically significant. All colored regions

are statistically significant. There are no statistically significant regions with white color. Note that while there is evidence for statistically significant trends in wind power density in some regions (panel a), there is little evidence for widespread trends in weather variability (panel b). The long-term trends in wind droughts (panel c) are nearly opposite in sign to the long-term trends in wind power density (panel a).

### Discussion

In this study, we conducted a historical analysis of the global distribution and trends in wind droughts from a purely geophysical perspective. We defined an energy deficit metric that integrates the depth and duration of wind droughts, to show places favorable for wind generation with low seasonal and weather

variability, and highlight any trends in these droughts. To calculate this energy deficit and reliably characterize wind resources and their historical trends, we used 44 years of wind speed, pressure, and temperature time series retrieved from reanalysis data. These wind speeds are provided at a 100-m height, which is consistent with the hub height of many modern wind turbines.

There are limitations to our analysis. The 100-m wind speeds obtained from reanalysis data can display a wide range of biases and errors that can be the effect of terrain orography, poor coverage of assimilated inputs, and model resolution<sup>23–25</sup>. The  $0.25^\circ \times 0.25^\circ$  spatial resolution (~30 km in the mid-latitudes) does not allow for consideration of the orographic effects of topography at this scale and below. The hourly time resolution does not allow to capture more extreme and rapid events, such as wind gusts, that may be important for voltage stability in electricity systems. Boundary layer parametrization related to the model representation of stability has been shown to be a cause for a substantial decrease in wind speed accuracy<sup>26</sup>. Furthermore, 44 years of data may not be enough to capture multidecadal wind variability. The Earth's atmosphere is characterized by different modes of variability that span large temporal and spatial scales. A study of German wind power generation highlighted the effect of a multidecadal maximum of wind energy generation that overlaps with some of the years of the reanalysis data<sup>27</sup>. This multidecadal variability cycle may lead to incorrect interpretation of long-term resource changes. Lastly, in our analysis, we assess wind droughts at the grid-cell level by considering only wind generation over year-long time periods. A spatial aggregation over large geographic regions may leverage the spatial and temporal variations in the occurrence of wind droughts in different grid cells to mitigate their overall impact<sup>28</sup>. A similar mitigation could be achieved by co-planning wind power with other generation technologies like solar to meet a variable electricity demand<sup>29</sup>.

Despite these limitations, our analysis provides insight into the wind resources of various regions. For example, we showed (Fig. 1) that the central parts of North America, southern parts of South America, and the central parts of Australia are characterized by relatively high power densities and low seasonal and weather variability. These regions are being and already have been exploited for electricity generation from wind. North American onshore wind installations accounted for about 155 GW in 2021 (contributing to 9% of the electricity generation), with the planned addition of about 46 GW over the following 5 years<sup>30</sup>; Argentina produced about 10% of its electricity from wind while Australia almost 12%<sup>3</sup>. Other parts of Asia, such as Turkmenistan and Tajikistan or some regions in Eastern Russia, are also characterized by favorable wind resources. In Africa, the Sahara and South Africa have relatively high power densities, and low seasonal and weather variability. The potential wind power of these regions in Asia and Africa remains mostly untapped in 2021.

The Central-to-Northwestern Europe region is characterized by relatively high power densities but relatively high seasonal and weather variability, which explains the higher probability of having severe wind droughts. Wind speed variability in Northwestern Europe is closely linked to the North Atlantic Oscillation, which is a prominent atmospheric mode that affects the strength and direction of westerly winds across the North Atlantic. Several studies have linked this oscillation as well as other Atlantic-European weather regimes, to over and under-generation from wind relative to the climatological seasonal mean<sup>28,31,32</sup>. Such variability and wind drought frequency may result in several system integration challenges for the large wind turbine fleets that are expected to be installed in those regions—for example, nine North Sea countries aim to install 120 GW of offshore capacity by 2030, and 300 GW by 2050<sup>33</sup>. To understand the potential order of magnitude of the impact of wind droughts, we can hypothesize a mean capacity factor of 0.4 for these installations, a representative, although probable, wind drought resulting in 400 h of energy deficit over an operational year, and temporal and spatial homogeneity of wind droughts in that region. The actual energy deficit incurred by such a 300-GW wind power system would then be of 48 TWh with respect to a power generation that follows the climatological seasonal cycle. This energy deficit would then need to be provided by energy storage or generation from other sources. For context, the total cumulative electrochemical battery and chemical storage capacity in the world up to 2021 amounted to about 16 GWh<sup>34</sup>.

The most pronounced trend in wind power densities is a broad increase over equatorial regions (Fig. 4). In contrast, India and Central Europe are characterized by decreasing power densities and increasing wind drought severity. Weather variability does not exhibit significant changes at the regional scale over the years of our analysis, although there is some evidence of decreasing variability over the Amazon region, small areas in North America, and Eastern Africa. Our results provide evidence for increasing wind drought severity in India and parts of Western Africa. Trends in annual mean wind power density play a more prominent role than changes in weather variability in most locations. Our analysis is unable to distinguish the extents to which observed trends are the result of anthropogenic climate change versus multidecadal natural variability, nor is it able to attribute trends to changing atmospheric modes. Regional variations in wind patterns can, in fact, be influenced by a combination of natural climate variability, human-induced climate change, and local and regional factors. Factors like land-use changes, aerosol pollution, and ocean-atmosphere interactions can also play a role in shaping wind speeds over specific regions. Further studies should aim to understand the complex interactions between natural variability and human-induced climate change in driving changes in the occurrence of wind droughts in selected regions.

The prevalence of wind droughts in the historical record, much of them in areas that historically did not have substantial amounts of wind power installations, combined with little evidence for strong trends in the prevalence of wind droughts, suggest a statistical analysis of weather reanalysis products could provide valuable guidance in designing wind-reliant electricity systems that are robust to the future wind droughts that will inevitably occur. For example, the energy deficit resulting from the most severe wind droughts in many places was between 2 and 3 times larger than the energy deficit resulting from the wind droughts of a typical year. This ratio overshadows any of the trends that we observed in the wind drought severity, which in most places in the world did not present any significant change.

Assessing the wind resource adequacy, its variability and long-term changes can provide strategic information for the sound and inclusive planning of future energy systems. Electricity systems will rapidly move into unprecedented territory, with intermittent renewable output gaining larger shares in the generation mix. This historical analysis of wind droughts can help to identify reliable locations for wind power generation and inform the optimal planning of energy storage facilities and other dispatchable generators needed to mitigate the worst impacts of severe wind droughts.

## Methods

To conduct our analysis, we used wind speeds, pressures, and temperatures retrieved from the ERA5 dataset<sup>35</sup>. ERA5 is produced by the Copernicus Climate Change Service (C3S) at the European Centre for Medium-Range Weather Forecasts (ECMWF). ERA5 is the fifth-generation ECMWF atmospheric reanalysis of the global climate covering the period from January 1940 to the present. It provides hourly estimates of a large number of atmospheric, land, and oceanic climate variables. The data cover the Earth on a regular latitude-longitude grid of 0.25 degrees (about 30 km in the mid-latitudes) and resolve the atmosphere using 137 levels from the surface up to a height of 80 km. We retrieved the 100-m components of wind speed, surface pressure, and 2-m temperature from January 1979 to December 2022 at hourly resolution, thus focusing our analysis on data that assimilate widespread satellite-based observations. This translates to about 400 billion data points for each of the four variables and about 3 TB of total data volume. From the wind speed time series, we estimate the power density time series. We then introduce an energy deficit metric to quantify the wind resource variability and wind droughts. The energy deficit metric quantifies the energy deficit of a wind-based power system over an annual time scale when we set a target generation profile. Note that the target generation profiles that we consider (constant or climatological) are aimed at characterizing the wind resource and variability and do not intend to represent the potential

complementarity of the wind generation profile with an actual electricity demand profile or power system. In the next paragraphs, we define each of the variables analyzed in this study and describe how we quantify them (see Supplementary Figs. 11, 12 for illustrative examples).

### Wind power density

For each grid cell, we calculate an hourly power density time series of the wind energy resource. The power density is the mean power available per square meter of swept area of a turbine. The 100-m wind power density time series,  $WPD(t)$ , is calculated as follows:

$$WPD(t) = 0.5 \frac{p(t)}{RT(t)} V(t)^3, \quad (1)$$

where  $p$  is the surface pressure,  $T$  the 2-m temperature in Kelvin,  $V$  the 100-m wind speed, and  $R$  the universal gas constant for dry air. Using the power density as a proxy for the wind resource does not allow us consideration of wind turbine wake effects or geophysical limits to the energy extraction<sup>36–38</sup>.

### Climatological seasonal wind power density

This quantity is obtained by averaging the same hour of all 44 years of the power density time series to obtain an hourly mean power density time series for each hour of the climatological year. In formulas,

$$CSWPD(t) = \frac{\sum_{y=1}^Y WPD_y(t)}{Y}, \quad (2)$$

where  $WPD_y$  is the wind power density time series in the year  $y$ , and  $Y$  is the number of years under consideration.

### Seasonal variability

For each grid cell, we calculate an energy deficit metric of seasonal variability that is related to the amount of storage that would be needed to supply constant generation from climatological mean hourly wind generation. We, therefore, consider a system that relies on the climatological seasonal power density time series ( $P_{\text{generation}}$ ) and aims to generate a constant profile ( $P_{\text{target}}$ ). Both the input and target generation are normalized to have a mean unit value. In formulas,

$$P_{\text{generation}}(t) = \frac{CSWPD(t)}{CSWPD_{\text{mean}}}, \quad (3)$$

$$P_{\text{target}} = 1, \quad (4)$$

where  $CSWPD_{\text{mean}}$  is the mean climatological seasonal wind power density.

### Weather variability

For each grid cell and year, we calculate an energy deficit metric of weather variability that is related to the amount of storage that would be needed to supply climatological mean hourly wind generation using the hourly power density time series in the year under consideration. We, therefore, consider a system that relies on the individual year power density time series ( $P_{\text{generation},y}$ ) and aims to generate the climatological seasonal profile ( $P_{\text{target}}$ ). We calculate an energy deficit for every one of the 44 years. Both the input and target generation are normalized to have a mean unit value in the year under consideration. In formulas,

$$P_{\text{generation},y}(t) = \frac{WPD_y(t)}{WPD_{y,\text{mean}}}, \quad (5)$$

$$P_{\text{target}}(t) = \frac{CSWPD(t)}{CSWPD_{\text{mean}}}, \quad (6)$$

where  $WPD_{y,\text{mean}}$  is the mean wind power density in year  $y$  and  $CSWPD_{\text{mean}}$  is the mean climatological seasonal wind power density.

### Wind drought

For each grid cell and year, we calculate an energy deficit metric for wind droughts that is related to the amount of storage that would be needed to provide climatological hourly generation from a system sized for the year with the least generation. We, therefore, consider a system that relies on the individual year power density time series ( $P_{\text{generation},y}$ ) and aims to generate the climatological seasonal profile ( $P_{\text{target}}$ ). We calculate an energy deficit for every one of the 44 years. In this case, the target generation is normalized to have a mean unit value, while the input generation is normalized to the year with the lowest mean power density. In formulas,

$$P_{\text{generation},y}(t) = \frac{WPD_y(t)}{\min_{y \in [1, Y]} (WPD_{y,\text{mean}})}, \quad (7)$$

$$P_{\text{target}}(t) = \frac{CSWPD(t)}{CSWPD_{\text{mean}}}. \quad (8)$$

The input generation has, therefore, a mean unit value only in that year, while it has greater mean values in other years. With this approach, we estimate the combined effect of changes in power density and weather variability on a system sized equally across all the years of our analysis. Note that having a system with a mean generation higher than the mean target generation in most of the years likely leads to conservative estimates of wind droughts.

### Energy deficit metric

To calculate our energy deficit metric (in hours of mean generation), we consider the time series of the integral of the generation balance:

$$E_{\text{deficit}}(t) = \int_0^t [P_{\text{target}}(\tau) - P_{\text{generation}}(\tau)] d\tau \quad \text{with } t \in [0, T], \quad (9)$$

where  $T$  is the period under consideration (e.g., 1 year). To fully capture the wind speed variability that may be present at the extremes of the period under consideration and that may go underestimated, we extend the time series of the target and input generation, i.e., we generate repeated time series of the target and input generation by concatenating two original time series. For example, if the original time series of the input generation has 8760 timesteps, the repeated time series of the input generation will have 17,520 timesteps, where the values from timestep 8761 to 17,520 will be the same as the ones from timestep 1 to 8760. Our energy deficit metric is the largest energy deficit present in the generation balance integral over the period under consideration:

$$E_{\text{deficit,max}} = \max_{t \in [0, T]} \left\{ E_{\text{deficit}}(t) - \min_{t_p \in [0, t]} [E_{\text{deficit}}(t_p)] \right\}. \quad (10)$$

### Data availability

100-m components of wind speed, surface pressure, and 2-m temperature from January 1979 to December 2022 at hourly resolution can be freely downloaded from the Copernicus's Climate Data Store at the following link: <https://cds.climate.copernicus.eu/cdsapp#!/dataset/reanalysis-era5-single-levels>. Postprocessed results, including wind power densities and energy deficits, can be freely downloaded from the following Zenodo repository: <https://zenodo.org/records/10082462>.

### Code availability

Python scripts that we wrote to process the ERA5 climate data, calculate wind power densities and energy deficits, and generate the figures are publicly available in the following GitHub repository: [https://github.com/eantonini/Global\\_wind\\_droughts](https://github.com/eantonini/Global_wind_droughts).

Received: 22 August 2023; Accepted: 6 February 2024;

Published online: 04 March 2024

## References

1. Our World In Data. Wind power generation, 2021. <https://ourworldindata.org/grapher/wind-generation>. (2022).
2. International Renewable Energy Agency (IRENA). Future of wind: deployment, investment, technology, grid integration and socio-economic aspects. (2019).
3. Our World In Data. Share of electricity production from wind. <https://ourworldindata.org/grapher/share-electricity-wind> (2023)
4. Bloomfield, H. What Europe's exceptionally low winds mean for the future energy grid. The Conversation. <https://theconversation.com/what-europes-exceptionally-low-winds-mean-for-the-future-energy-grid-170135>
5. European Centre for Medium-Range Weather Forecasts (ECMWF). Low winds. <https://climate.copernicus.eu/esotc/2021/low-winds>
6. Rife, D., Krakauer, N., Coha, D., & Collier, J. C. A new kind of drought: U.S. record low windiness in 2015. IEEE Earthzine. <https://earthzine.org/a-new-kind-of-drought-u-s-record-low-windiness-in-2015/> (2022).
7. Lledó, L., Bellprat, O., Doblas-Reyes, F. J. & Soret, A. Investigating the effects of Pacific sea surface temperatures on the wind drought of 2015 over the United States. *J. Geophys. Res. Atmos.* **123**, 4837–4849 (2018).
8. The Western Electricity Coordinating Council (WECC). State of the Interconnection Report. (2016).
9. Shekhar, J., Saji, S., Agarwal, D., Ahmed, A. & Joseph, T. Assessing and planning for variability in India's wind resource. (2021).
10. Leahy, P. G. & McKeogh, E. J. Persistence of low wind speed conditions and implications for wind power variability. *Wind Energy* **16**, 575–586 (2013).
11. Patlakas, P., Galanis, G., Diamantis, D. & Kallos, G. Low wind speed events: persistence and frequency. *Wind Energy* **20**, 1033–1047 (2017).
12. Ruhnau, O. & Qvist, S. Storage requirements in a 100% renewable electricity system: extreme events and inter-annual variability. *Environ. Res. Lett.* <https://doi.org/10.1088/1748-9326/ac4dc8> (2022).
13. Pryor, S. C. & Barthelmie, R. J. Climate change impacts on wind energy: a review. *Renew. Sustain. Energy Rev.* **14**, 430–437 (2010).
14. Pryor, S. C., Barthelmie, R. J. & Kjellstro, E. Potential climate change impact on wind energy resources in northern Europe: analyses using a regional climate model. *Clim. Dyn.* **25**, 815–835 (2005).
15. Reyers, M., Moemken, J. & Pinto, J. G. Future changes of wind energy potentials over Europe in a large CMIP5 multi-model ensemble. *Int. J. Climatol.* **36**, 783–796 (2016).
16. Bloom, A., Kotroni, V. & Lagouvardos, K. Climate change impact of wind energy availability in the Eastern Mediterranean using the regional climate model PRECIS. *Nat. Hazards Earth Syst. Sci.* **8**, 1249–1257 (2008).
17. Tobin, I. et al. Climate change impacts on the power generation potential of a European mid-century wind farms scenario. *Environ. Res. Lett.* <https://doi.org/10.1088/1748-9326/11/3/034013> (2016).
18. Pryor, S. C. et al. Wind speed trends over the contiguous United States. *J. Geophys. Res.* **114**, D14105 (2009).
19. Karnauskas, K. B., Lundquist, J. K. & Zhang, L. Southward shift of the global wind energy resource under high carbon dioxide emissions. *Nat. Geosci.* **11**, 38–43 (2018).
20. Pryor, S. C., Schoof, J. T. & Barthelmie, R. J. Winds of change?: projections of near-surface winds under climate change scenarios. *Geophys. Res. Lett.* **33**, L11702 (2006).
21. Vautard, R., Cattiaux, J., Yiou, P., Thépaut, J. N. & Ciais, P. Northern Hemisphere atmospheric stilling partly attributed to an increase in surface roughness. *Nat. Geosci.* **3**, 756–761 (2010).
22. Bloomfield, H. C. et al. Quantifying the sensitivity of European power systems to energy scenarios and climate change projections. *Renew. Energy* **164**, 1062–1075 (2021).
23. Rose, S. & Apt, J. What can reanalysis data tell us about wind power? *Renew. Energy* **83**, 963–969 (2015).
24. Rose, S. & Apt, J. Quantifying sources of uncertainty in reanalysis derived wind speed. *Renew. Energy* **94**, 157–165 (2016).
25. González-Aparicio, I. et al. Simulating European wind power generation applying statistical downscaling to reanalysis data. *Appl. Energy* **199**, 155–168 (2017).
26. Davidson, M. R. & Millstein, D. Limitations of reanalysis data for wind power applications. *Wind Energy* **25**, 1646–1653 (2022).
27. Wohland, J., Omrani, N., Eddine, Keenlyside, N. & Witthaut, D. Significant multidecadal variability in German wind energy generation. *Wind Energy Sci.* **4**, 515–526 (2019).
28. Grams, C. M., Beerli, R., Pfenniger, S., Sta, I. & Wernli, H. Balancing Europe's wind-power output through spatial deployment informed by weather regimes. *Nat. Clim. Change* **7**, 557–562 (2017).
29. Antonini, E. G. A., Ruggles, T. H., Farnham, D. J. & Caldeira, K. The quantity-quality transition in the value of expanding wind and solar power generation. *iScience* **25**, 104140 (2022).
30. Mordor Intelligence. North America wind power market size and share analysis - growth trends & forecasts (2023–2028). (2022).
31. Garrido-Perez, J. M., Ordóñez, C., Barriopedro, D., García-Herrera, R. & Paredes, D. Impact of weather regimes on wind power variability in western Europe. *Appl. Energy* **264**, 114731 (2020).
32. Laurila, T. K., Sinclair, V. A. & Gregow, H. Climatology, variability, and trends in near-surface wind speeds over the North Atlantic and Europe during 1979–2018 based on ERA5. *Int. J. Climatol.* **41**, 2253–2278 (2021).
33. Henley, J. European countries pledge huge expansion of North Sea wind farms. <https://www.theguardian.com/environment/2023/apr/24/european-countries-pledge-huge-expansion-of-north-sea-wind-farms> (2023).
34. U. S. D. of Energy. DOE global energy storage database. <https://sandia.gov/ess-ssl/gesdb/public/index.html>
35. Hersbach, H. et al. The ERA5 global reanalysis. *Q. J. R. Meteorol. Soc.* **146**, 1999–2049 (2020).
36. Antonini, E. G. A., Romero, D. A. & Amon, C. H. Optimal design of wind farms in complex terrains using computational fluid dynamics and adjoint methods. *Appl. Energy* **261**, 114426 (2020).
37. Antonini, E. G. A. & Caldeira, K. Atmospheric pressure gradients and Coriolis forces provide geophysical limits to power density of large wind farms. *Appl. Energy* **281**, 116048 (2021).
38. Antonini, E. G. A. & Caldeira, K. Spatial constraints in large-scale expansion of wind power plants. *Proc. Natl Acad. Sci. USA* **118**, e2103875118 (2021).

## Acknowledgements

All authors acknowledge the financial support from Gates Ventures LLC through a gift provided to the Carnegie Institution for Science.

## Author contributions

Enrico Antonini and Ken Caldeira designed the study. Enrico Antonini performed the retrieval, processing, and analysis of the dataset with support from Lei Duan and Ken Caldeira. Enrico Antonini generated the figures with support from Edgar Virgúez, Tyler Ruggles, and Ken Caldeira. Edgar Virgúez generated Supplementary Fig. 12 with support from Enrico Antonini and Ken Caldeira. Enrico Antonini wrote the paper with input from Edgar Virgúez, Sara Ashfaq, Lei Duan, Tyler Ruggles, and Ken Caldeira.

## Competing interests

Edgar Virgúez is a member of the Duke University Board of Trustees. The remaining authors declare no competing interests. The views and opinions



expressed in this manuscript are those of the authors and do not necessarily reflect the views or positions of their institutions.

### Additional information

**Supplementary information** The online version contains supplementary material available at <https://doi.org/10.1038/s43247-024-01260-7>.

**Correspondence** and requests for materials should be addressed to Enrico G. A. Antonini.

**Peer review information** *Communications Earth & Environment* thanks Anasuya Gangopadhyay and the other, anonymous, reviewer(s) for their contribution to the peer review of this work. Primary Handling Editors: Martina Grecequet. A peer review file is available.

**Reprints and permissions information** is available at <http://www.nature.com/reprints>

**Publisher's note** Springer Nature remains neutral with regard to jurisdictional claims in published maps and institutional affiliations.

**Open Access** This article is licensed under a Creative Commons Attribution 4.0 International License, which permits use, sharing, adaptation, distribution and reproduction in any medium or format, as long as you give appropriate credit to the original author(s) and the source, provide a link to the Creative Commons licence, and indicate if changes were made. The images or other third party material in this article are included in the article's Creative Commons licence, unless indicated otherwise in a credit line to the material. If material is not included in the article's Creative Commons licence and your intended use is not permitted by statutory regulation or exceeds the permitted use, you will need to obtain permission directly from the copyright holder. To view a copy of this licence, visit <http://creativecommons.org/licenses/by/4.0/>.

© The Author(s) 2024